Supporting Information

Frühholz et al. 10.1073/pnas.1411315112

SI Materials and Methods

Stimulus Material and Trial Sequence.

Experiment 1: Voice-selective responses in auditory cortex. We used 8-s sound clips taken from an existing database (1) to identify common and distinct regions in the bilateral STC that are sensitive to human voices in each group of patients. To this end, we used sound clips representing 20 sequences of human voices and 20 sequences of animal or environmental sounds. Each sound clip was presented once. The scanning sequence also contained twenty 8-s silent events. The patients had to listen to these stimuli passively.

Experiment 2: Emotional and attentional responses in auditory cortex (dichotic listening). To identify the brain region for the processing of vocal emotions, we used stimulus material that consisted of four speech-like, but semantically meaningless, words ("molen," "belam," "nikalibam," and "kudsemina") taken from an existing database (16-bit, 44-kHz sampling rate) (2). Each word was spoken in either a neutral or angry tone by two male and two female speakers (3). Angry voices were used because they had already been used in previous studies with a similar paradigm in healthy individuals (4, 5) and because they produce reliable activation of the amygdala (6) and the corticosubcortical networks involved in emotional vocalization processing (3, 7). Furthermore, angry voices are among the best-recognized emotions in the vocal modality (8). Auditory stimuli had a mean duration of 690 ms and were equated for mean sound pressure levels. During scanning, auditory stimuli were presented with MRI-compatible headphones (MR confon GmbH) at ∼70 dB of sound pressure level. The same word was presented simultaneously to the left ear and the right ear in a dichotic listening paradigm, but it was spoken by different speakers (4, 5). For two blocks, participants had to attend to the left ear only, but for another two blocks, they had to listen to the right ear only. Their task was to judge the gender (male or female) for the voice of the attended ear. They answered by pressing buttons with their right index and middle fingers (response button assignment was counterbalanced across patients).

The experimental design consisted of three conditions: (*i*) an angry voice was presented to the attended ear, and a neutral voice was presented to the unattended ear (*an* trials); (*ii*) a neutral voice was presented to the attended ear, and an angry voice was presented to the unattended ear (*na* trials); and (*iii*) neutral voices were presented to both ears (*nn* trials). The same paradigm has previously been used to study the effect of attention and emotion on both cortical and amygdalar activity in response to vocal emotions in healthy individuals (4, 5).

Each experimental block consisted of 72 trials, resulting in a total of 288 trials. Each stimulus spoken by one speaker was presented in combination with a stimulus from the other speaker. The speaker identities, as well as the angry and neutral utterances, were counterbalanced for the attended and unattended ears. Trials were presented in randomized order, except that the same speaker, a speaker of the same gender, and the same emotion of the voice on the *an* trials were allowed to appear no more than three times in a row. The same rules applied to the sequence of voices on the unattended ear, with the additional rule that the speaker identity of the voice in the unattended ear was never allowed to match the speaker identity of the voice in the attended ear. Each dichotic auditory stimulus was preceded by a visual fixation cross (1° × 1°) on a gray background, presented for 1.25 ± 0.25 s before auditory onset and remaining on the screen for the same duration as the auditory stimulus. After the auditory stimulus, an empty gray screen was presented for 4 ± 1 s, during which time participants were asked to make a gender decision as fast and as accurately as possible.

Image Acquisition. For experiments 1 and 2, we recorded imaging data on a 3-T Siemens Trio TIM System by using a T2*-weighted gradient echo-planar imaging sequence. We used continuous whole-head acquisition of 36 slices [thickness/gap = 3.2/0.64 mm, field of view (FoV) = 205 mm, in-plane 3.2 × 3.2 mm] aligned to anterior commissure-posterior commissure plane with a time to repetition (TR)/time to echo (TE) of 2.1 s/0.03 s. Finally, a high-resolution magnetization prepared rapid acquisition gradient echo T1-weighted sequence (192 contiguous 1-mm slices, TR/TE/time to inversion = 1.9 s/2.27 ms/900 ms, FoV = 296 mm, in-plane 1 × 1 mm) was obtained in sagittal orientation to record structural brain images from each subject.

Image Analysis. We used statistical parametric mapping (SPM) software (version 8; Welcome Department of Cognitive Neurology, London, United Kingdom) for preprocessing and statistical analysis of functional images from experiments 1 and 2. Functional images were realigned and coregistered to the anatomical image. We used the Clinical toolbox (www.mccauslandcenter.sc.edu/CRNL/clinical-toolbox) to segment and normalize patients' anatomical scans to the MNI space by using a unified segmentation approach (9) with the DARTEL toolbox implemented in SPM version 8. Brain segmentation was performed after including lesion masks drawn on the patients' anatomical scans for cost function masking (10). Individual DARTEL flow fields for normalization were estimated from segmented gray matter (GM) and white matter (WM) tissue classes. During normalization, functional images were resampled to a 2-mm^3 voxel size and spatially smoothed by using an isotropic Gaussian kernel of 6 mm^3 FWHM, and GM images with an original resolution of 1 mm^3 were spatially smoothed with a kernel of 8 mm^3. The normalized and smoothed GM images were used for a VBM analysis, in which GM voxels reflect the absolute amount of brain volume. We specifically examined the GM volume in the healthy amygdala in both MTL patient groups by using an anatomical mask of the individually segmented amygdala (below).

We used a general linear model for the first-level statistical analyses of functional data, with boxcar functions defined by the onset and duration of the auditory stimuli. These boxcar functions were convolved with a canonical hemodynamic response function. Separate regressors were created for each experimental condition. Six motion correction parameters were also included as regressors of no interest to minimize false-positive activations that were due to task-correlated motion.

For experiment 1 (cortical voice responses), we contrasted vocal against nonvocal animal and environmental stimuli at a threshold of $P < 0.005$ (uncorrected) and a cluster extent of $k = 67$ voxels corresponding to $P < 0.05$ corrected at the cluster level. This combined voxel and cluster threshold corresponds to $P < 0.05$ corrected at the cluster level and was determined by the 3DClustSim algorithm implemented in AFNI software (afni.nimh.nih.gov/afni) according to the estimated smoothness of the data across all contrasts. The cluster extent threshold of $k = 67$ was the maximum value for the minimum cluster size across contrasts of both experiments. We determined voice-sensitive regions along the STG and STS in both hemispheres. To increase the statistical power across patients groups and to avoid any spurious activity in contralesional temporal brain areas, we flipped all functional contrast images for the right MTL group along the *y*–*z* plane. Thus, all functional activations in one (left)

hemisphere represent ipsilesional activity, whereas the functional activations in the other (right) hemisphere represent contralesional activity. As for the dichotic listening experiment, we flipped contrast images for right MTL patients along the *y*–*z* plane.

For experiment 2 (emotional responses during dichotic listening), linear contrasts for each participant were created by comparing all anger trials (*an* + *na*) with *nn* trials (*an* + *na* > *nn*), *an* trials with *nn* trials (*an* > *nn*), and *na* trials with *nn* trials (*na* > *nn*). All contrasts were masked with an inclusive binary mask of the GM and WM brain tissue of each patient, excluding the lesioned brain area. These contrasts were taken to a second-level random effects group analysis to compare functional activity between left and right MTL patients. As for experiment 1, we flipped contrast images for right MTL patients along the *y*–*z* plane. All activation maps in Figs. 2–4 for right MTL patients were reflipped along the *y*–*z* plane for illustration purposes. All resulting statistical maps were thresholded with a combined voxel and cluster threshold of $P < 0.005$ (uncorrected) and a minimum cluster extent of $k = 67$ (above).

ROI analyses were performed on anatomically defined regions in the healthy (left or right) amygdala for all patients. We used the automated brain segmentation procedure as implemented in FreeSurfer software (11) to determine an anatomical mask of the intact amygdala in native space in each patient. These amygdala masks were then normalized to MNI space using the DARTEL flow fields. Beta estimates extracted from the healthy amygdala were subjected to a 2 × 3 repeated-measure ANOVA, with the between-subject factor group (left or right) and the within-subject factor condition (*an*, *na*, or *nn*). Functional ROIs were 3-mm radius spheres around peak activations that resulted from the main analysis.

We performed a functional connectivity analysis by using activity in the left fOP as the seed region common to both the left and the right patient groups (Fig. 4). The functional connectivity analysis was set up as a PPI analysis (12) using a general linear model for each of the seed regions, including three regressors. The first regressor was the extracted and deconvolved time course of functional activity in a seed region (physiological variable). The second regressor was the comparison between angry and neutral voices during the explicit task (psychological variable); that is, we created a time course regressor for the comparison of task conditions, including as many sampling points as for the physiological variable. Finally, the third regressor in our PPI included the interaction between the first two regressors. This interaction was created by a point-by-point multiplication of the time course for the physiological variable and the time course for the psychological variable. The last regressor was the only regressor of interest, whereas the psychological variable and the deconvolved time course served as regressors of no interest in each PPI analysis. The inclusion of the first two regressors ensures that the resulting functional activation is determined solely by the interaction between the physiological variable and the psychological variable. Data for angry (*an* + *na*) trials compared with *nn* trials, for the *an* trials compared with *nn* trials, and for *na* trials compared with *nn* trials were entered into separate PPI analyses. All resulting statistical maps were thresholded by a combined voxel and cluster threshold of $P < 0.005$ (uncorrected) and a cluster extent of $k = 67$ (above).

SI Results

Similar to the ANOVA analysis of the behavioral data as reported for the dichotic experiment in the main text, we performed an additional ANOVA on RTs and error rates (%). The data were analyzed by a repeated-measure ANOVA with the between-subject factor group (left MTL patients, right MTL patients) and the within-subject factors laterality (attend left ear, attend right ear) and condition (angry voice presented to the attended ear, angry voice presented to the unattended ear, neutral voices in both ears). However, additionally, we took the lesion size of the patient as a covariate into account to test the influence of the lesion size on the behavioral data.

There was no effect of laterality ($F_{1,17} = 0.315$, $P = 0.582$) and group ($F_{1,18} = 0.020$, $P = 0.890$) on RTs. However, RTs differed across conditions ($F_{2,34} = 4.096$, $P = 0.025$), and Bonferroni corrected pairwise comparisons indicated longer response latencies for *an* trials compared with both *na* trials ($P < 0.001$) and *nn* trials ($P = 0.002$). There were no significant interactions between experimental factors for RTs (all $F < 1.649$, all $P > 0.216$).

Similarly, error rates showed a significant difference only between conditions ($F_{1,17} = 7.093$, $P = 0.003$), with more errors for *an* trials compared with both *na* ($P < 0.001$) and *nn* ($P < 0.001$) trials (all after Bonferroni corrected post hoc comparisons). The factors laterality and group were not significant, and no interaction between factors reached significance (all $F < 1.470$, all $P > 0.242$).

1. Belin P, Zatorre RJ, Lafaille P, Ahad P, Pike B (2000) Voice-selective areas in human auditory cortex. *Nature* 403(6767):309–312.
2. Bänziger T, Scherer KR (2010) Introducing the Geneva Multimodal Emotion Portrayal (GEMEP) corpus. *Blueprint for Affective Computing: A Sourcebook*, eds Bänziger T, Scherer KR, Roesch EB (Oxford Univ Press, Oxford), pp 271–294.
3. Frühholz S, Ceravolo L, Grandjean D (2012) Specific brain networks during explicit and implicit decoding of emotional prosody. *Cereb Cortex* 22(5):1107–1117.
4. Sander D, et al. (2005) Emotion and attention interactions in social cognition: Brain regions involved in processing anger prosody. *Neuroimage* 28(4):848–858.
5. Grandjean D, et al. (2005) The voices of wrath: Brain responses to angry prosody in meaningless speech. *Nat Neurosci* 8(2):145–146.
6. Fruhholz S, Grandjean D (2013) Amygdala subregions differentially respond and rapidly adapt to threatening voices. *Cortex* 49(5):1394–1403.
7. Frühholz S, Grandjean D (2012) Towards a fronto-temporal neural network for the decoding of angry vocal expressions. *Neuroimage* 62(3):1658–1666.
8. Patel S, Scherer KR, Björkner E, Sundberg J (2011) Mapping emotions into acoustic space: The role of voice production. *Biol Psychol* 87(1):93–98.
9. Ashburner J, Friston KJ (2005) Unified segmentation. *Neuroimage* 26(3):839–851.
10. Andersen SM, Rapcsak SZ, Beeson PM (2010) Cost function masking during normalization of brains with focal lesions: Still a necessity? *Neuroimage* 53(1):78–84.
11. Fischl B, et al. (2002) Whole brain segmentation: Automated labeling of neuroanatomical structures in the human brain. *Neuron* 33(3):341–355.
12. Friston KJ, et al. (1997) Psychophysiological and modulatory interactions in neuroimaging. *Neuroimage* 6(3):218–229.

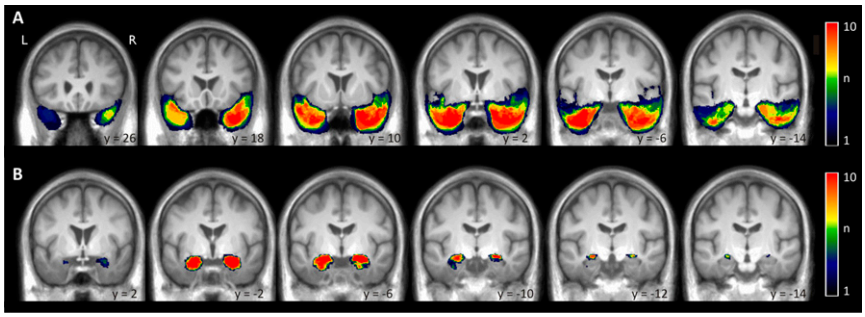

Fig. S1. (*A*) Overlay of normalized lesion masks for left and right MTL patients. The anatomical overlap varies between lesions from one up to 10 left or right MTL patients. (*B*) Overlays of normalized brain masks for the intact amygdala resulting from automatized brain segmentation. The left amygdala mask results from brain segmentation of the right MTL patients, and vice versa for the right amygdala masks.

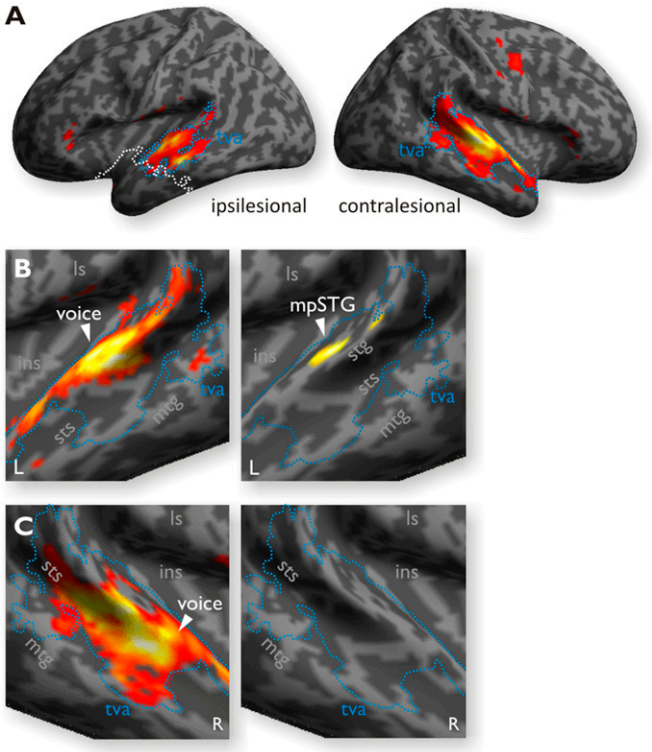

Fig. S2. (*A*) Results of the voice sensitivity experiment (experiment 1) for vocal compared with nonvocal sounds, taking into account the individual lesion size that overlapped with Brodmann areas (BAs) 21, 22, and 38. The lesion overlap was included as a covariate in the analysis and treated as an additional regressor of no interest, which, however, is able to explain variance. Please note that the blue outline of the voice-sensitive area is taken from the analysis without the covariate for the purpose of comparison between both types of analysis. (*B*, *Left*) In right MTL patients, comparing voices relative to nonvocal sounds showed extended activity in the left STG. (*B*, *Right*) When comparing right MTL patients relative to left MTL patients, voices produced significantly higher activity in the mpSTG. (*C*) In left MTL patients, comparing voices relative to nonvocal sounds showed extended activity in the right STG (*Left*), but no regions showed higher activity in left MTL patients compared with right MTL patients (*Right*). This finding indicates that the original activation found in the right STC seems to be associated with the lesion extent in the lateral STC, because the lesion overlap could explain a considerable amount of variance in this region such that the original activation disappeared. ins, insula; L, left; ls, lateral sulcus; mtg, middle temporal gyrus; R, right; tva, temporal voice area.

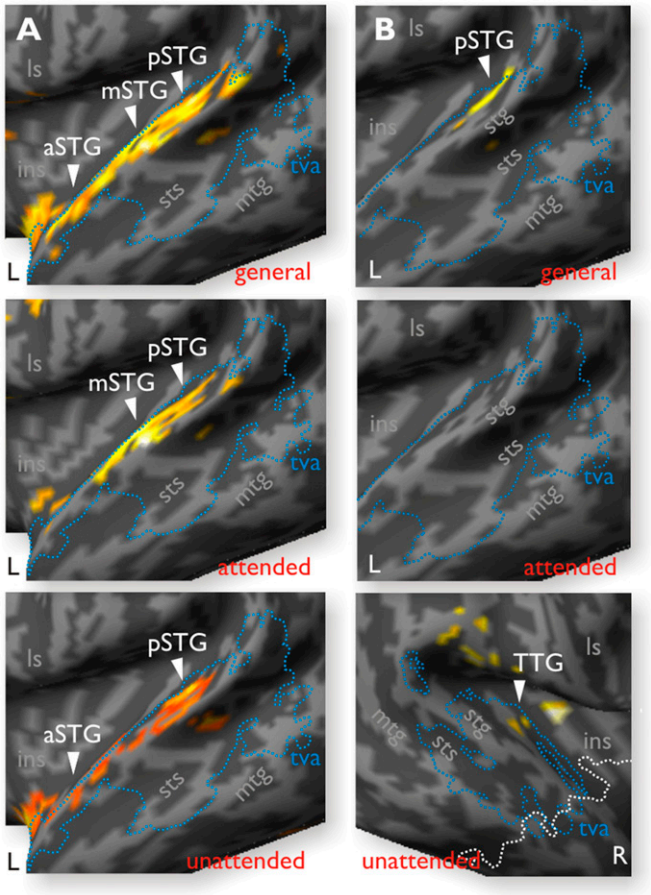

Fig. S3. Functional activations in the dichotic listening experiment taking into account the individual lesion size in BAs 21, 22, and 38. (*A*) Right MTL patients had significant increased activity in the left STG for angry (*an* + *na*) trials compared with *nn* trials (general, *Upper*), as well as for *an* trials (*Middle*) and *na* trials (*Lower*) taken separately. (*B*) Direct comparison between left and right MTL patients revealed significantly increased activity in the left pSTG for all angry (*an* + *na*) trials (general), in the right TTG for *na* trials, but not in the left mSTG for *an* trials. Thus, the original level of activity in left mSTG seems to be associated with the lesion size in the lateral STC.

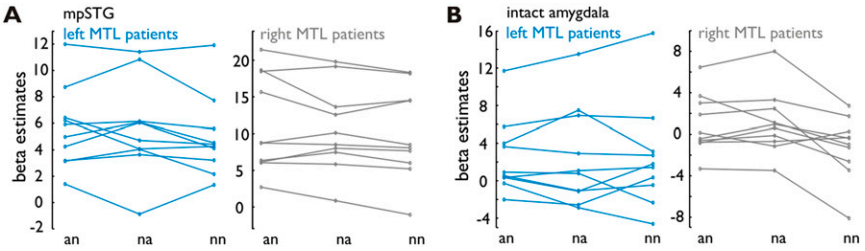

Fig. S4. Beta estimates in the left mpSTG (*A*) and the intact amygdala (*B*) plotted separately for each left and right MTL patient. Although right MTL patients show relatively consisting increases for emotional (*an* and *na*) trials compared with *nn* trials, no such effects were found for left MTL patients.

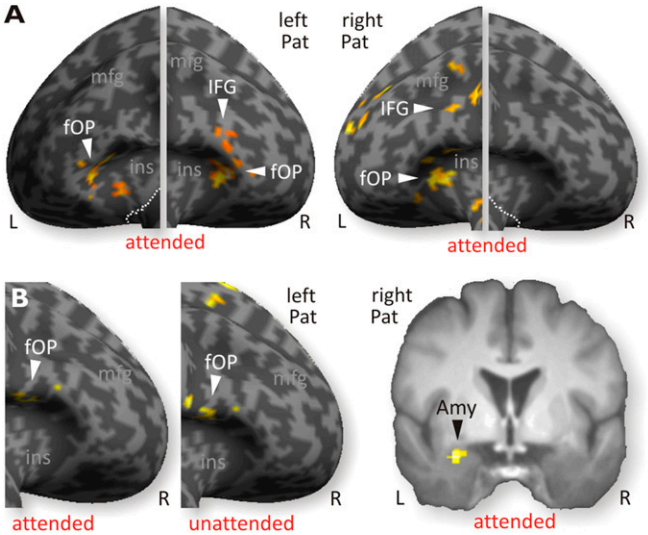

Fig. S5. Functional activations and functional connectivity in the dichotic listening experiment taking into account the individual lesion size in BAs 21, 22, and 38. (*A*, *Left*) Left MTL patients (Pat) showed activations to angry voices in bilateral IFC, especially for *an* trials. (*A*, *Right*) For the same trials, right MTL patients showed activity only in the left IFC. (*B*, *Right*) PPI analysis using the left fOP as a seed region revealed higher functional connectivity with the left amygdala for right MTL patients during *an* trials but not during *na* trials. (*B*, *Left*) In left MTL patients, connectivity of the left fOP increased with the right IFC only, during both *an* and *na* trials, but not with the amygdala.

Table S1. Demographic and seizure-related data for left and right MTL patients

Patient	Lesion side	Gender	Age, y	Age of seizure onset, y	Months after surgery
1	Left	Male	23	7	120
2	Left	Male	67	49	113
3	Left	Female	37	1.5	56
4	Left	Female	68	37	93
5	Left	Female	25	8	47
6	Left	Male	50	4	124
7	Left	Male	36	14	75
8	Left	Female	64	6	78
9	Left	Female	25	4	88
10	Left	Male	47	25	144
11	Right	Male	31	4	72
12	Right	Male	43	7	105
13	Right	Male	50	8	112
14	Right	Male	25	18	17
15	Right	Male	31	20	9
16	Right	Female	38	25	11
17	Right	Female	68	30	122
18	Right	Male	37	13	100
19	Right	Female	32	30	8
20	Right	Female	53	4	96

Table S2. Peak activations for all anger (*an* + *na*) trials compared with *nn* trials for left MTL patients (*A*) and for right MTL patients (*B*) and functional activity for anger compared with neutral voices (*C*)

Region	Cluster size	z value	MNI		
			x	*y*	*z*
(*A*) Left MTL patients					
Right IFG	221	4.01	36	30	2
		4.01	40	34	−2
		3.99	40	26	2
		3.29	30	26	6
(*B*) Right MTL patients					
Right cingulate gyrus	423	4.10	10	32	28
		3.94	0	32	26
		3.50	0	42	20
Right medial/superior frontal gyrus	186	4.67	14	12	60
		3.56	20	10	58
		3.43	8	4	64
Left IFG	1,776	4.17	−34	32	0
		4.14	−44	16	−12
Left medial frontal gyrus	174	3.99	−6	18	48
		3.14	−4	24	56
		3.11	8	16	48
Left middle frontal gyrus	200	3.85	−18	52	16
		3.55	−26	44	16
		3.15	−18	42	6
Left STG		4.65	−66	−36	12
		4.22	50	0	−4
		4.03	−60	−10	0
		3.91	−50	−12	4
Right STG	187	4.00	56	−12	2
Right TTG		3.92	46	−16	6
		3.57	40	−20	8
Right STG		3.52	50	−8	6
Left superior parietal lobule	115	3.72	−12	−58	58
		3.16	−14	−56	66
		2.80	−14	−64	64
Left cingulate gyrus	80	3.63	−4	−6	42
		3.39	−2	−12	44
		2.87	4	−12	40
Left fusiform gyrus	149	3.54	−26	−56	0
		3.42	−36	−50	−2
		2.89	−38	−42	−6
Right lingual gyrus	70	3.95	20	−88	−14
Right fusiform gyrus	133	3.48	−38	−48	−28
		3.09	−32	−52	−26
Right fusiform gyrus	67	3.23	−24	−76	−22
		3.20	−26	−68	−24
		3.11	−20	−72	−26
Right pallidum	88	3.51	12	−6	8
Right pallidum		2.82	18	4	16
(*C*) Right vs. left MTL patients					
Right cingulate gyrus	118	3.92	−4	−6	42
		3.33	8	−26	38
		3.30	4	−18	38
Left STG	81	3.72	−50	−36	16
		3.21	−52	−28	8
		2.95	−54	−24	6
		2.62	−50	−20	2
Left fusiform gyrus	111	3.22	−34	−50	−4
		3.19	−26	−54	−2
		3.08	−24	−54	6
Right superior occipital gyrus	180	3.83	22	−86	38
		3.65	10	−86	40
		3.55	10	−88	36

Functional activity for anger compared with neutral voices was significantly higher in right MTL patients compared with left MTL patients. Please note that in the following tables, after functional images for right MTL patients were flipped along the *y*–*z* plane, we report the reflipped peak activation for right MTL patients such that they correspond to their original hemispheric occurrence.

Table S3. Functional activity for an trials compared with *nn trials* for left MTL patients (*A*) and for right MTL patients (*B*), functional activity for *an* trial voices compared with *nn* trial voices (*C*), functional activity for *na* trials compared with *nn* trials in right MTL patients (*D*), and functional activity for *na* trials compared with *nn* trials (*E*)

Region	Cluster size	z value	MNI		
			x	*y*	*z*
an vs. *nn* trials					
(*A*) Left MTL patients					
Right STG	187	4.69	12	14	44
Left IFG	333	4.09	−38	20	2
		3.75	−38	32	0
		3.71	−40	40	−2
		3.71	−40	28	−2
Right IFG	315	4.29	44	32	0
		3.95	36	32	0
		3.52	40	26	2
		3.20	52	26	10
Right medial frontal gyrus		3.97	8	28	36
		3.77	6	16	46
		3.12	8	18	52
(*B*) Right MTL patients					
Left middle frontal gyrus	145	3.42	−18	54	18
		3.42	−26	36	24
		3.05	−26	42	24
Left precentral gyrus		3.13	−42	−2	30
		3.01	−40	2	28
Left medial frontal gyrus	851	3.92	−6	16	46
		3.88	12	10	60
		3.83	12	34	30
Left IFG		3.56	−32	32	−2
		3.51	−32	24	4
Left IFG	188	3.31	−44	10	32
		3.31	−42	16	40
Left STG	531	3.89	−60	−8	0
		3.76	−54	−12	4
		3.15	−56	−2	−2
		3.14	−54	−22	6
Left temporal pole	444	3.68	−44	16	−12
Left insula		3.47	−32	18	4
Left fusiform gyrus	83	3.23	−32	−52	−28
Left fusiform gyrus	110	3.18	−24	−60	0
		2.97	−30	−56	4
		2.96	−36	−50	0
Left superior parietal lobule	86	3.13	−18	−70	46
		3.01	−16	−66	56
		2.86	−20	−58	66
(*C*) Right vs. left MTL patients					
Left STG	70	3.41	−42	−6	4
		2.67	−34	0	2
Left STG	68	3.36	−60	−10	0
		3.14	−54	−14	2
		2.78	−54	−20	4
Left lingual gyrus	102	3.10	−24	−54	6
		2.97	−28	−52	4
		2.88	−38	−54	6
na vs. *nn* trials					
(*D*) Right MTL patients					
Right cingulate gyrus	105	4.17	4	28	22
		3.68	2	32	24
		3.30	8	32	26
Left STG	710	4.51	−36	8	−16
		3.98	−52	−26	6
		3.81	−50	0	−4

Table S3. Cont.

Region	Cluster size	z value	MNI		
			x	*y*	*z*
		3.75	−46	2	−12
Right STG	114	4.03	58	−30	20
		3.97	58	−20	16
Right TTG	128	3.73	38	−18	8
Right STG		3.43	56	−12	2
		3.09	46	−16	6
Right inferior parietal lobule		3.10	60	−30	32
		2.95	58	−22	30
Right fusiform gyrus		3.15	42	−46	−20
(*E*) Right vs. left MTL patients					
Right TTG	84	3.94	38	−16	8
Right STG		2.99	42	−12	8
		2.94	34	−26	16
Right TTG		2.88	38	−24	16
Right inferior parietal lobule	118	3.68	60	−34	26
		3.65	60	−32	18
Right postcentral gyrus		3.19	58	−22	18
Right inferior parietal lobule		3.10	58	−24	32
Right superior occipital gyrus	105	3.46	22	−86	36
		3.21	12	−88	38

In *D*, functional activity for *an* trial voices compared with *nn* trial voices was significantly higher in right MTL patients compared with left MTL patients. In *E*, functional activity for *na* trials compared with *nn* trials was significantly higher in right MTL patients compared with left MTL patients.

Table S4. Functional activity for the PPI analysis including the left fOP as a seed region: Peak activations for *an* compared with *nn* trials for left MTL patients (*A*), functional activity for anger compared with neutral voices in left vs. right MTL patients (*B*) and in right vs. left MTL patients (*C*), and peak activations for *na* trials compared with *nn* trials for left vs. right MTL patients (*D*)

Region	Cluster size	z value	MNI		
			x	*y*	*z*
an vs. *nn* trials					
(*A*) Left MTL patients					
Right IFG	141	4.44	44	14	2
		3.77	54	8	10
		3.39	52	12	8
(*B*) Left vs. right MTL patients					
Right IFG	175	4.25	44	12	2
		3.87	50	14	6
		3.73	56	10	10
		3.65	54	18	16
Left cingulate gyrus	141	3.61	−4	34	20
		3.50	4	32	20
		3.15	0	26	32
(*C*) Right vs. left MTL patients					
Left amygdala	33	3.35	−28	2	−20
na vs. *nn* trials					
(*D*) Left vs. right MTL patients					
Right superior frontal gyrus	73	3.71	14	14	50
		3.66	14	18	56
Right IFG	134	3.51	42	14	2
		3.32	50	10	−2
		3.28	56	14	12
		2.93	54	2	14
Right superior frontal gyrus	70	3.24	2	8	64
		3.04	−2	4	62

Functional activity for anger voices compared with neutral voices was significantly higher in left MTL patients compared with right MTL patients (*B*), as well as higher in right MTL patients compared with left MTL patients (*C*). In *D*, peak activations for *na* trials compared with *nn* trials revealed activity for left MTL patients compared with right MTL patients.